A

correlation, r	tH	CTH	tK	CTK
tH	1.00			
CTH	0.99	1.00		
tK	0.61	0.71	1.00	
CTK	0.80	0.87	0.96	1.00

B

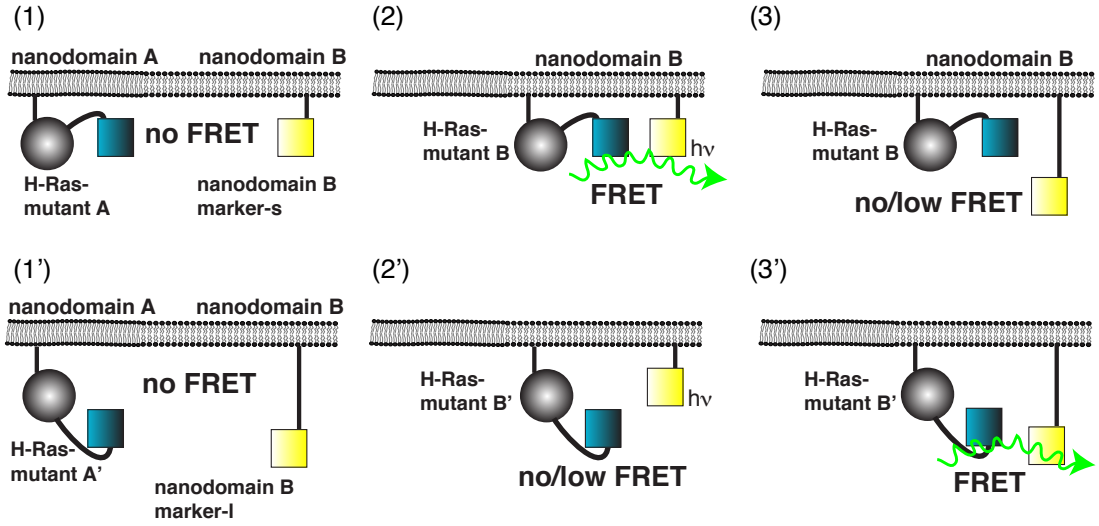

C

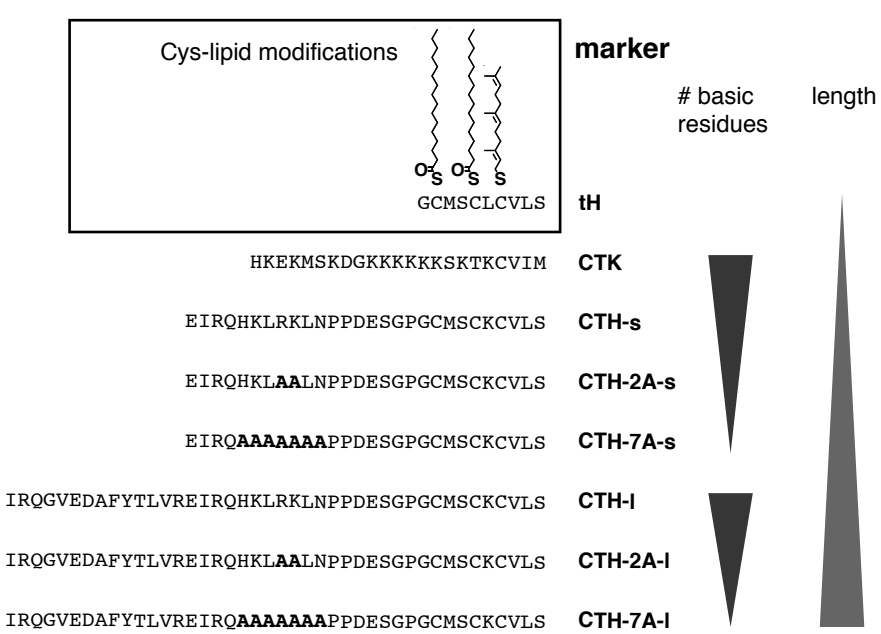

Supplementary Figure S1

A

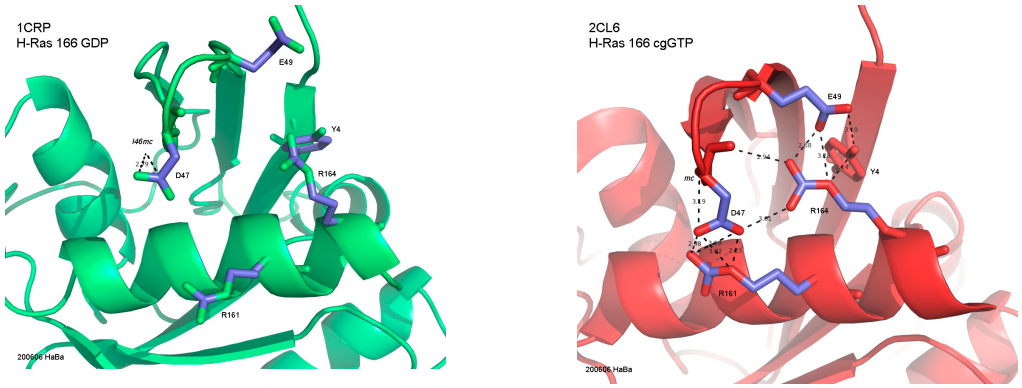

B

mutant GTP-H-ras

correlation, r	R169/K170A	R169/K170/ R128/R135A	R128/R135A	R161/R164A	D47/E49A	D47A	R161A
R169/K170A							
R169/K170/R128/R135A	0.814						
R128/R135A	0.661	0.328					
R161/R164A	0.714	0.296	0.932				
D47/E49A	0.574	0.310	0.871	0.827			
D47A	0.261	0.000	0.740	0.665	0.935		
R161A	0.151	-0.341	0.622	0.633	0.357	0.361	

mutant GDP-H-ras

correlation, r	R169/K170A	R169/K170/ R128/R135A	R128/R135A	R161/R164A	D47/E49A	D47A	R161A
R169/K170A							
R169/K170/R128/R135A	0.299						
R128/R135A	0.707	0.423					
R161/R164A	0.219	0.878	0.310				
D47/E49A	0.133	0.676	0.000	0.743			
D47A	1.000	0.299	0.707	0.219	0.133		
R161A	0.543	0.596	0.768	0.555	0.000	0.543	

C

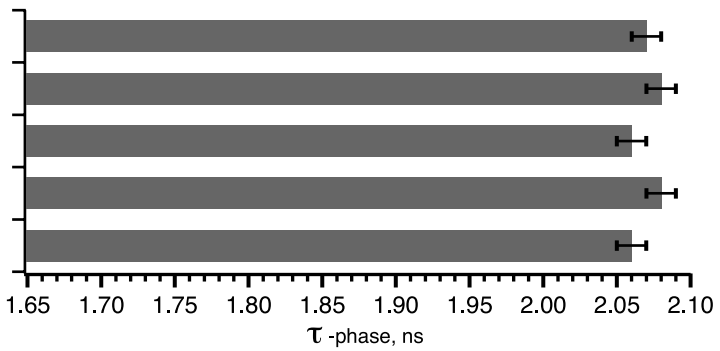

Supplementary Figure S2

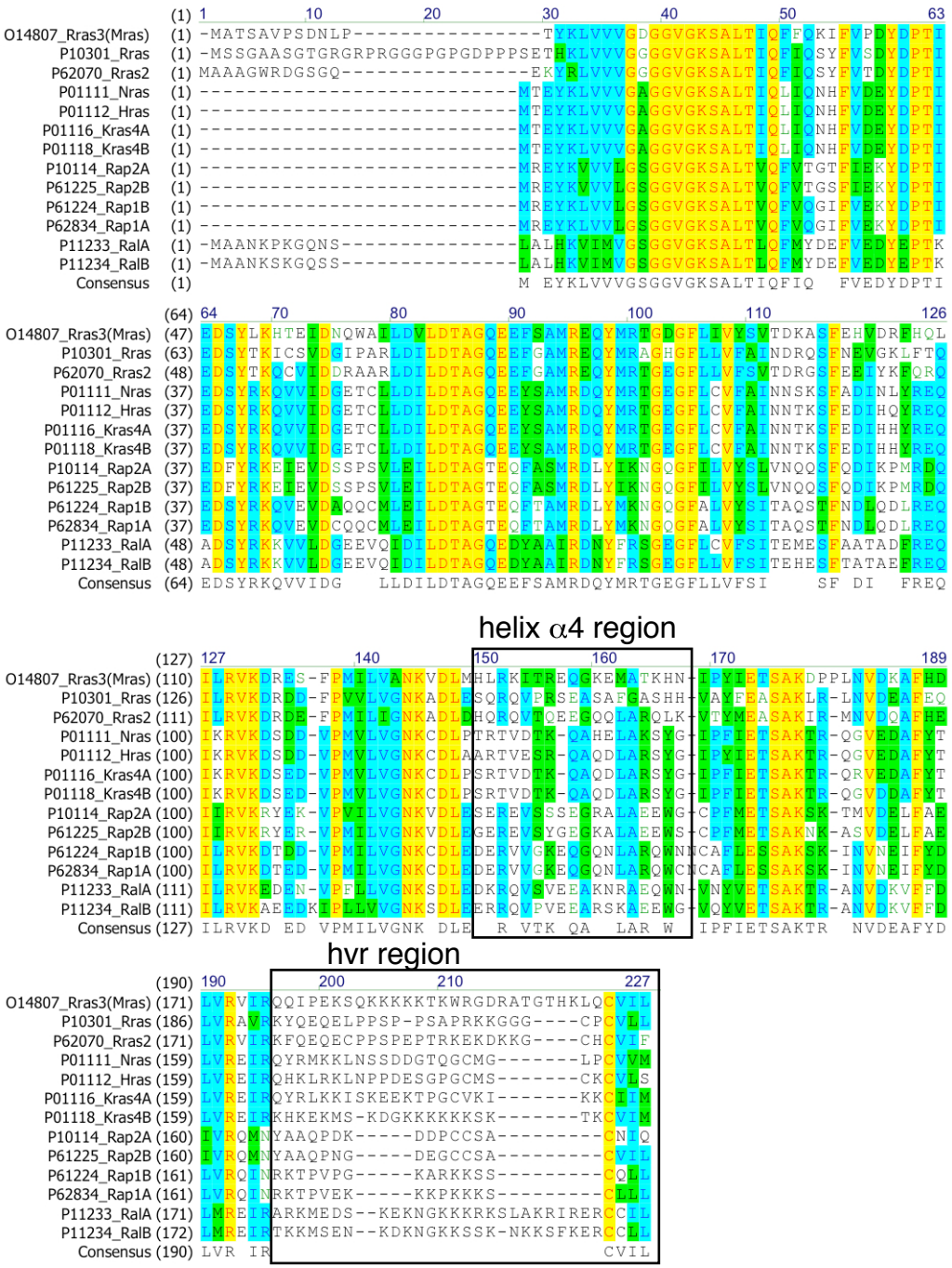

Supplementary Figure S3

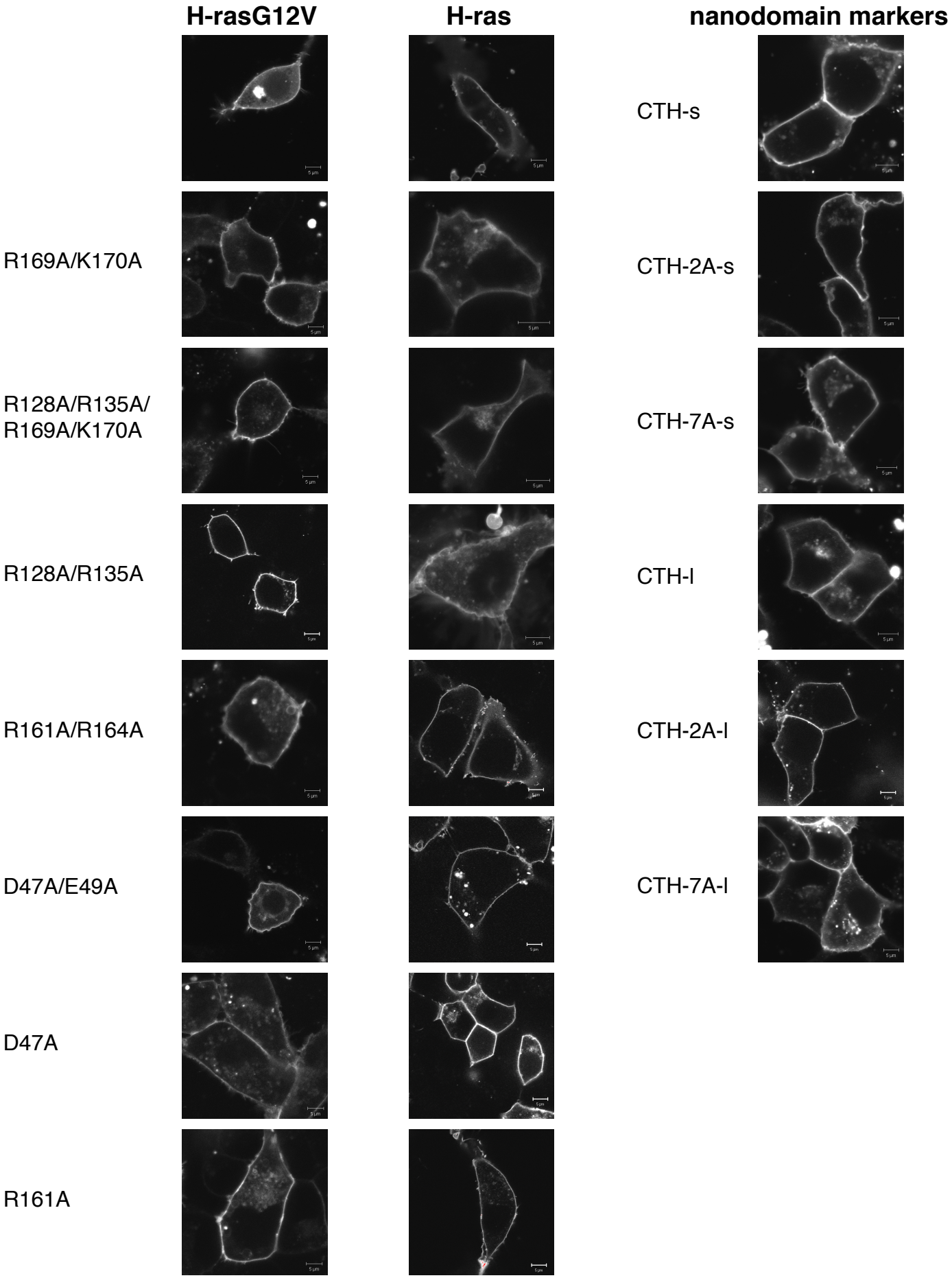

Supplementary Figure S4

Supplementary Material

Supplementary Figure S1

(A) Correlation coefficient matrix of FRET-vectors shown in Figure 1D. **(B)** Initial, naïve FRET-scenarios explaining our orientation and lateral segregation (together: membrane organization) sensitive FRET approach. Full length H-ras in two conformational states (e.g. GTP or GDP) is probing nanodomains labelled with nanodomain-markers of different lengths. If H-ras and nanodomain marker are laterally segregated into different nanodomains, no FRET can occur, irrespective of H-ras conformation or length of the nanodomain marker (1 and 1'). However, if they are in the same nanodomain, FRET may be possible only in one conformational state (2) with the short version of the nanodomain marker, but not the other (2'). Conversely, the longer version of the nanodomain marker may lead to FRET only with the conformation in (3'), but not in (3). (**C**) Amino acid sequences used to construct *bona fide* nanodomain markers by fusing them to the C-terminus of fluorescent proteins. These sequences were all derived from the C-terminus of H-ras. As the MD-simulations (Figure 2A, B) also indicated proximity changes of parts of H-ras relative to the membrane, we designed two sets of H-ras derived nanodomain markers. The shorter set with extension '–s' was derived from residues 162-189 of H-ras and the longer set with extension '–l' was derived from residues 149-189. Previous data suggested that varying the number of basic residues of membrane anchors modifies lateral segregation properties (Abankwa & Vogel, 2007). Therefore, each set contained the unmutated HVR of H-ras (CTH), and two mutants with a decreasing number of basic residues. In the nanodomain marker CTH-2A only two specific basic residues, R169 and K170 were substituted by alanines, while in CTH-7A the first half of the HVR was substituted by alanines. Residues R169 and K170 were mutated, as they were suggested to interact with the membrane in the GDP-model (Gorfe et al, 2007). Moreover, these residues are phylogenetically well conserved in the classical Ras-isoforms H-, N- and K-ras, in the p21-clade of the Ras-subfamily (supplementary information Figure S3). On the other hand, we used the Δ1ala-mutation as a template for CTH-7A, where the first half of the HVR is replaced by alanines. This mutation altered nanoclustering of the full length GTP-H-ras to become cholesterol sensitive (Rotblat et al, 2004). We complemented our set of markers by including the complete HVR (residues 166-188) of K-ras, which

contained the highest number of basic residues. In the box, palmitoyls and the farnesyl lipid modifications are shown at the cysteines of H-ras that become covalently modified with these lipids.

Supplementary Figure S2

(**A**) Crystal structures of GDP- (left) and GTP-(right) H-ras show residues of the putative membrane-orientation switch region. When comparing all x-ray structures of GTP- and GDP-bound H-ras, we noticed in the region adjacent to the HVR that residues D47, E49 in the β2-β3-loop and R161 and R164 on helix α5 are differently arranged in the two structures. This suggested that these residues relax with different constraints, depending on whether GTP or GDP is bound. We reasoned that these constraints would at least partially pertain to membrane bound H-ras. Accession numbers of representative structures are as shown. (**B**) Correlation coefficient matrices for reduced FRET-vectors of full length GTP-(top) and GDP-H-ras mutants (bottom). To calculate the coefficients of GDP-H-ras-R161A, it was assumed that the E_{max} of GDP-H-ras-R161A/CTH-2A-l was insignificantly changed. (**C**) HEK 293 cells transiently coexpressed mGFP-tagged H-rasG12V mutants. Using FLIM, the average donor (mGFP) -fluorescence lifetimes determined from the phase-shift are shown with their s.e.m. Data from three independent experiments were pooled and no statistically significant differences between the lifetimes of the mutants and that of H-rasG12V were found, using 2-tailed Student's t-test.

Supplementary Figure S3

Sequence alignment of the 13 Ras isoforms of the p21 Ras-subfamily (given with SwissProt accession numbers) reveals that the sequence corresponding to helix α4 is the second least conserved extended sequence stretch after the HVR (both boxed). Note the abundance of basic residues in both regions, which may potentially form contacts with the acidic lipid head groups. Amino acids are abbreviated in one-letter code. Sequence alignment was done in AlignX from the Vector NTI sofware package (Invitrogen). Highlighting denotes sequence conservation, with yellow -100% conservation, blue-identity and green-conservative exchanges.

Supplementary Figure S4

Predominant plasma membrane localization of H-ras was unaffected by introduced mutations. Confocal imaging of live BHK or HEK293 cells expressing fluorescent protein tagged H-ras mutants and novel nanodomain markers as indicated. Scale bars are 5μm.

References

Abankwa D, Vogel H (2007) A FRET map of membrane anchors suggests distinct microdomains of heterotrimeric G proteins. *J Cell Sci* 120: 2953-2962

Gorfe AA, Bayer M-H, Abankwa D, Hancock JF, McCammon JA (2007) Structure and dynamics of the full-length lipid-modified H-Ras protein in a 1,2-dimyristoylglycero-3-phosphocholine bilayer. *J Med Chem* 50: 674-684

Rotblat B, Prior IA, Muncke C, Parton RG, Kloog Y, Henis YI, Hancock JF (2004) Three separable domains regulate GTP-dependent association of H-ras with the plasma membrane. *Mol Cell Biol* 24: 6799-6810